

36 **1. Introduction**

37 Afforestation is one of the most frequently debated strategies to mitigate the impacts of the
38 anthropogenic climate change (Sonntag et al., 2016; Harper et al., 2018; Roe et al., 2019), because
39 forests are able to remove large amounts of CO₂ from the atmosphere during their growth and store
40 the carbon long-term in their biomass (Luyssaert, et al., 2010; Pan et al., 2011). Besides this beneficial
41 biogeochemical effect on the global greenhouse effect, afforestation is also changing the
42 biogeophysical characteristics of the land surface (Pielke et al., 2011; Bright et al., 2017). For instance,
43 the evapotranspiration potential of forests is generally higher than of other vegetation types (Zhang
44 et al., 2001), due to a higher biomass and a deeper root system. Thus, a comparatively large part of
45 the incoming solar radiation is transformed into latent heat instead of heating up the land surface
46 (Strandberg & Kjellström, 2019). This effect of afforestation is particularly relevant in regions with large
47 amounts of available energy for evapotranspiration, like the tropics. Therefore, afforestation is known
48 to have a regional cooling effect in the tropics (Lawrence & Vandecar, 2015; Zeppetello et al., 2020).
49 On the other hand, the surface albedo of forests is lower in comparison to other vegetation types
50 (Bonan, 2008). A larger part of the incoming solar radiation is absorbed, and thus more energy is
51 available to heat up the land surface. This albedo effect is further intensified by the presence of snow,
52 since forests are only partially masked by snow, while other vegetation types are completely covered
53 and reflect more solar radiation (Essery, 2013). The snow masking effect is therefore especially
54 important in the high latitudes, where the land surface is over a large part of the year covered with
55 snow. Afforestation has consequently a regional warming effect in the high latitudes (Bala et al., 2007,
56 Li et al., 2015, Duveiller et al., 2018).

57 In the mid-latitudes, both the increased turbulent heat transport (sensible + latent) and the albedo
58 effect are relevant (Bonan, 2008). In this geographical area, solar radiation is sufficiently available and
59 thus, the albedo effect has a major impact on the regional climate conditions. In addition, the energy
60 and water supply are generally high in the mid-latitudes, and the increased evaporative potential with
61 afforestation has consequently an important effect on the surface energy balance. The arising question
62 whether afforestation leads to a warming or a cooling of the regional climate conditions in Europe is
63 therefore subject of current research and scientific discussions (e.g. Breil et al., 2023a).

64 Recent studies indicate that afforestation in Europe leads to a warming in winter, due to the snow
65 masking effect of forests (Lejeune et al., 2017; Davin et al., 2020). In this season, large parts of the land
66 surface are covered with snow in the mid-latitudes, and thus more solar radiation is absorbed by
67 forests than by other vegetation types. In summer, surface temperatures are generally reduced, while
68 boundary layer temperatures are increased with afforestation (Breil et al., 2020). Because of the higher
69 surface roughness of forests in comparison to other vegetation types, the increased solar radiation
70 with afforestation is efficiently transformed into sensible heat and transported away from the surface

71 into the atmosphere (Lee et al., 2011; Burakowski et al., 2018). Atmospheric temperatures are
72 consequently increased, and surface temperatures are reduced, although more solar radiation is
73 absorbed (Breil et al., 2020). Moreover, the commonly higher evapotranspiration rates of forests
74 increase the moisture content in the atmosphere and can therefore increase downwind precipitation
75 sums in Europe (Meier et al., 2021).

76 These effects of afforestation in the mid-latitudes are generally derived either from point
77 measurements of adjacent eddy covariance stations in forests and grasslands (e.g. Lee et al., 2011),
78 from satellite data (e.g. Li et al., 2015), from coarsely resolved global climate simulations (e.g. Bala et
79 al., 2007), or from idealized modeling studies (e.g. Davin et al., 2020). However, it is not possible on
80 the basis of these methods to quantify the effects of afforestation on the regional climate conditions
81 in the mid-latitudes. Although satellite data provide a high spatial coverage, they are not suitable to
82 analyze the underlying land-atmosphere interactions. Such interactions can be investigated with point
83 measurements of flux towers, but the arising atmospheric feedback processes cannot be analyzed with
84 such observations. While all these processes can be simulated with global climate models, the spatial
85 resolution of these simulations is generally too low to investigate all relevant processes in the
86 necessary detail. Although regional climate simulations have higher resolution, regional climate
87 models were until now, to our knowledge, only applied in idealized afforestation scenarios (e.g. Davin
88 et al., 2020; Breil et al., 2020). The actual effects of afforestation on the regional climate conditions in
89 Europe are therefore not yet comprehensively analyzed. This is especially the case for the impact of
90 afforestation on the European climate trend since the 1980s. During this period, the strongest
91 temperature increase in the last 2000 years took place (Gulev et al., 2021), while at the same time, the
92 forest cover increased comparatively strong.

93 Therefore, the goal of this study is to quantify how strong afforestation affected the regional climate
94 conditions during this period of intense regional warming in Europe, by considering the actual
95 afforestation between 1986-2015 in higher resolved simulations with a Regional Climate Model (RCM).
96 In this RCM experiment, a simulation is performed in which all land use changes during this 30 year
97 period (including afforestation) are implemented, and compared to an RCM simulation in which
98 afforestation is not considered. In this way, we are able to explicitly quantify the impact of
99 afforestation on the recent climate conditions in Europe, and analyze whether afforestation regionally
100 counteracted the general climate trend by e.g., an increased evapotranspiration rate and an enhanced
101 turbulent heat exchange, or if the increased absorption of solar radiation with afforestation even
102 intensified the regional climate trend in Europe.

103 The design of the modeling experiment is described in section 2. In section 3, the local (section 3.1)
104 and non-local (section 3.2) effects of afforestation on the climate conditions in Europe are assessed,

105 with a special focus on extremes (section 3.3) and climate variability (section 3.4). Results are discussed
106 in section 4 and conclusions are drawn in section 5.

107

108 **2. Methods**

109 **2.1. Model simulations**

110 In the framework of this study, regional climate simulations with the RCM COSMO-CLM (CCLM, Rockel
111 et al., 2008) coupled to the Land Surface Model VEG3D (Breil & Schädler, 2021) are used to analyze
112 the impact of afforestation on the regional climate conditions in Europe between 1986-2015. The
113 simulations are performed for the Coordinated Downscaling Experiment – European Domain (EURO-
114 CORDEX; Jacob et al., 2014) on a horizontal resolution of 0.11° (~12.5 km). The simulations are driven
115 by the ERA5 reanalysis (Hersbach et al., 2020) at the lateral boundaries and the lower boundary over
116 sea. The simulation period is 1986–2015, with a spin-up of 7 years before 1986.

117 During the first simulation, yearly updated land use maps of the land cover conditions in Europe are
118 implemented in CCLM-VEG3D in which all historical land use changes between 1986-2015 are
119 considered, excluding afforestation (Fig. 1a). This experiment constitutes the reference simulation
120 (REF). In the second simulation, the same land use dataset is used as in REF, but now afforested areas
121 are additionally implemented (AFF). Fig. 1b shows all grid cells, in which afforestation took place
122 between 1986-2015.

123 The underlying land use dataset was developed within the Land Use and Climate Across Scales (LUCAS)
124 project (Davin et al., 2020), based on the European Space Agency Climate Change Initiative Land Cover
125 (ESA-CCI LC) dataset (European Space Agency, 2017). The yearly changes in the land use map during
126 the simulation period are derived from the Land-Use Harmonization 2 (LUH2) dataset (Hurtt et al.,
127 2020). More information on how the applied land use map was constructed can be found in Hoffmann
128 et al., (2022).

129 In CCLM-VEG3D, only the dominant land use class in a grid cell is considered. Thus, afforestation is only
130 considered in our model setup in grid cells in which forest is becoming the dominant land use class.
131 The land use information in these grid cells is then completely assigned to forest. Although the spatial
132 resolution of the grid cells is rather small in our modeling experiment, this results in an overestimation
133 of the forest fraction in afforested grid cells. In return, afforested areas in which forest is not the
134 dominant land use class are not considered and the forest fraction is consequently underestimated in
135 the model.

136 By comparing the results of the AFF simulation with the results of the REF simulation, the effects of
137 afforestation on the regional climate conditions in Europe during the simulation period are assessed.
138 For the analysis, we differentiate between local effects and non-local effects. As local effects, we define
139 changes in the climate conditions in a grid cell in which afforestation took place. A non-local effect is

140 defined as a change in the climate conditions in non-afforested areas, which is indirectly caused by
141 changes in the surface energy balance in afforested grid cells. The statistical significance of the
142 temperature changes in AFF in comparison to REF is calculated with a Wilcoxon-Rank-Sum-Test, a non-
143 parametric statistical test analyzing the differences between two paired datasets.

144 Beside the effects of afforestation on the general climate conditions in Europe, we also investigate its
145 impact on climate extremes and the interannual climate variability. Changes in heat extreme
146 intensities are expressed as differences in the days above the 90th percentile of the daily maximum
147 temperatures in 2 m height in summer (JJA). In this context, we define the heat period intensities as
148 the mean daily maximum 2 m temperature for these warmest 10 % of summer days, and compare
149 these mean values for AFF and REF with each other. Changes in cold extreme intensities are expressed
150 as differences in the mean daily maximum 2 m temperature for the coldest 10 % of winter days (DJF).
151 Effects on the climate variability are analyzed by calculating the standard deviation of the mean
152 seasonal surface temperatures.

153

154 **2.2. Afforested areas**

155 According to the land use dataset derived in the LUCAS project (Hoffmann et al., 2022), about 1.1% of
156 the land mass in the EURO-CORDEX domain was afforested during the period 1986-2015. By converting
157 these land use change information into CCLM-VEG3D with its dominant land use class approach, about
158 1,7% of the CCLM-VEG3D model domain was afforested. These land use changes were not
159 homogeneous and evenly distributed, but were carried out on small-scales and on isolated locations.
160 In Figure 1, all regions in CCLM-VEG3D are shown which were afforested during the 30 year period in
161 Europe. Larger areas were afforested in the Balkan region, central and north-eastern Europe, while in
162 Scandinavia and south-eastern Europe almost no afforestation took place. All over Europe, 63% of the
163 afforested areas were converted from croplands, 31% from grasslands.

164 The main differences in the vegetation characteristics between different forest types and croplands
165 and grasslands are summarized in table 1. While the surface albedo of forests is lower and the surface
166 roughness is higher, croplands and grasslands are characterized by a shallow root system and a lower
167 leaf area index (LAI). In this context, the vegetation characteristics of different deciduous tree species
168 (e.g. beech, oak, etc.) and different coniferous tree species (pine, spruce, etc.) are all combined in one
169 representative forest class, respectively. This means that for the different vegetation parameters,
170 describing the characteristics of these different tree species, the mean values over the parameter
171 space of the respective deciduous and coniferous trees are used. In CCLM-VEG3D, therefore, only one
172 deciduous forest class and one coniferous forest class are considered. For the deciduous forest class,
173 only deciduous broadleaved trees are taken into account, while in the coniferous forest class, only

174 evergreen needleleaved trees are included. Evergreen broadleaved trees (e.g., Mediterranean oaks)
175 or deciduous needleleaved trees (e.g. larch) are consequently not considered.

176

177 **3. Results**

178 First, we analyze the capability of CCLM-VEG3D to reproduce the general climate conditions in Europe.
179 Figure 2 shows the differences between the reference simulation (REF) and the ERA5-Land reanalysis
180 (Muñoz-Sabater et al., 2021) for (a) the yearly mean 2 m temperatures and (b) the yearly total
181 precipitation sums during the period 1986-2015.

182 A warm bias is simulated over most parts of Europe in the reference simulation, extending from
183 Southern Europe over Central Europe to Eastern Europe. However, these deviations to ERA5-Land are
184 in the same range as the biases of other RCMs, as demonstrated by Kotlarski et al., (2014). Regarding
185 Northern Europe and the British Isles, the simulation results agree well with the reanalysis data.

186 Total precipitation sums are underestimated in CCLM-VEG3D in southern and western Europe, but
187 overestimated in eastern and parts of northern Europe (shown as a percentual deviation in Fig. 2). This
188 is also true for the mountainous regions of the Pyrenees and the Alps. On the other hand, the simulated
189 precipitation sums agree well with the reanalysis data over large parts of Central and Eastern Europe
190 as well as of southern Scandinavia. Thus, the results of CCLM-VEG3D reflect the already known
191 precipitation pattern of regional climate simulations with CCLM (Kotlarski et al., 2014).

192 Therefore, although a certain model bias for the simulated 2 m temperature and the total precipitation
193 sums is found, the simulation results of CCLM-VEG3D are comparable with the results of other RCMs
194 (Kotlarski et al., 2014) and we conclude that the model is generally able to reproduce the general
195 climate conditions in Europe.

196

197 **3.1. Local effects**

198 **3.1.1 Winter**

199 The local effects of afforestation in Europe on different components of the surface energy balance are
200 analyzed for the period 1986-2015 (Figure 3). Since afforestation in Europe took place only on small-
201 scales and on isolated locations, local effects are summarized for three geographical sub-regions,
202 northern Europe (NE), central Europe (CE) and southern Europe (SE) for visualization purposes, which
203 are highlighted in Figure 1.

204 In winter, an important change with afforestation is that trees (particularly coniferous trees) maintain
205 a dense vegetation throughout the whole season (characterized by a high leaf area index (LAI)), while
206 the original vegetation types have only a low vegetation cover (especially croplands). Therefore,
207 forests are generally able to transpire more water than grasslands and particularly croplands during

208 winter (Fig. 3b). As a consequence, more energy is transformed into latent heat and less energy is
209 transformed into sensible heat in forests (Fig. 3c).

210 This feature is especially pronounced in central Europe. Within the period 1986-2015, mean local latent
211 heat fluxes were increased about 5.1 W/m^2 in winter (Fig. 3b), while mean local sensible heat fluxes
212 were reduced about -5.5 W/m^2 (Fig. 3c). At the same time, mean local net short-wave radiation was
213 slightly increased about 0.7 W/m^2 (Fig. 3a), leading to a positive surface energy budget ($+1.1 \text{ W/m}^2$,
214 Fig. 3d). Thus, afforestation led in central Europe to a slight local warming in winter for the period
215 1986-2015 ($+0.2 \text{ K}$, Fig. 4a).

216 The same processes were also simulated in northern Europe. The mean local latent heat fluxes in
217 winter were increased ($+1.9 \text{ W/m}^2$, Fig. 3b), while the mean local sensible heat fluxes were reduced ($-$
218 2.3 W/m^2 , Fig. 3c). The increase in the mean local net short-wave radiation was with 0.1 W/m^2 (Fig.
219 3a) even smaller than in central Europe. The impact of the reduced surface albedo on the mean
220 radiative energy input, associated with the snow masking effect of forests in winter, must therefore
221 be rather small. The generally low insolation in this season consequently impeded stronger differences
222 in the mean local radiative energy input in central and particularly in northern Europe. As a
223 consequence, the surface energy budget was slightly increased in northern Europe ($+0.5 \text{ W/m}^2$, Fig.
224 3d) and the mean warming with afforestation was small ($+0.1 \text{ K}$, Fig. 4a).

225 Since the general insolation in southern Europe in winter is higher than in central and northern Europe,
226 a comparatively strong increase in the mean local net short-wave radiation was simulated with
227 afforestation ($+2.0 \text{ W/m}^2$, Fig. 3a), due to the lower albedo values. Therefore, one could assume that
228 this enhanced radiative energy input should also have led to the strongest temperature increase in
229 Europe during winter. But this is not the case. On the contrary, afforestation resulted in a slight
230 reduction of the mean local surface temperature in southern Europe in winter within the simulated 30
231 year period (-0.1 K , Fig. 4a). This is because in southern Europe, not only the mean local latent heat
232 fluxes were increased with afforestation ($+2.7 \text{ W/m}^2$, Fig. 3b), but also the mean local sensible heat
233 fluxes were high and on a level comparable to croplands and grasslands (-0.1 W/m^2 , Fig. 3c). That
234 means the increased local radiative energy input was transformed into high latent heat fluxes as well
235 as high sensible heat fluxes. As a result, the surface energy budget was slightly negative (-0.6 W/m^2 ,
236 Fig. 3d), resulting in a slight local cooling in southern Europe in winter (Fig. 4a).

237 Although these slight temperature changes in northern, central and southern Europe can be explained
238 consistently with changes in the surface energy budget, the local temperature effects of afforestation
239 are statistically not significant in winter, as calculated by a Wilcoxon-Rank-Sum-Test at a 95 % level.
240 Thus, random causes for the temperature changes cannot be excluded.

241

242 **3.1.2 Summer**

243 In summer, the most striking effect of afforestation is the general increase in absorbed solar radiation.
244 The mean local net short-wave radiation was increased all over Europe within the period 1986-2015
245 (Fig. 3a). However, this increased radiative energy input at the surface did not result in a warming of
246 the surface temperatures. Because of the higher surface roughness of forests in comparison to
247 croplands and grasslands (table 1) the absorbed solar radiation is, in general, more efficiently
248 transformed into turbulent heat with afforestation (e.g. Breil et al., 2020). Therefore, both the mean
249 local latent heat fluxes and the mean local sensible heat fluxes were enhanced in all subregions (Fig.
250 3b+c). As a result, more energy was released as turbulent heat into the atmosphere than was
251 additionally absorbed by solar radiation. Thus, the surface energy budget became negative (Fig. 3d),
252 although the mean local net short-wave radiation was increased. Afforestation led consequently to a
253 cooling of the mean local surface temperatures all over Europe in summer for the period 1986-2015
254 (Fig. 4b).

255 The strongest cooling was simulated in southern Europe, with a mean temperature reduction of -0.8 K
256 (Fig. 4b). However, at single locations, the cooling was pronounced more strongly. The maximum
257 cooling effect was about -3.1 K, with 20 % of the afforested areas showing a mean cooling of more
258 than -1.3 K with afforestation. This strong cooling was reached, although the albedo effect of
259 afforestation was highest in southern Europe, due to the high solar altitude in summer. But the
260 increase in mean local net short-wave radiation of 5.0 W/m^2 (Fig. 3a) was completely counteracted by
261 a considerably increased mean local sensible heat flux ($+11.0 \text{ W/m}^2$, Fig. 3c) and a slightly increased
262 mean local latent heat flux ($+0.6 \text{ W/m}^2$, Fig. 3b). The comparatively small increase in latent heat fluxes
263 and the pronounced increase in sensible heat fluxes were caused by the generally low soil water
264 contents in summer and the resulting soil moisture limitation of evapotranspiration in southern Europe
265 (Seneviratne et al., 2010).

266 In central and northern Europe, the soil moisture limitation in summer was not as strongly pronounced
267 as in southern Europe. The mean local latent heat fluxes were consequently on a higher level ($+4.9$
268 W/m^2 in CE and $+3.3 \text{ W/m}^2$ in NE, Fig. 3b), although the additional radiative energy input with
269 afforestation was not as high as in southern Europe ($+4.1 \text{ W/m}^2$ in CE and $+ 2.9 \text{ W/m}^2$ in NE, Fig. 3a).
270 Since the mean local sensible heat fluxes were also increased ($+2.1 \text{ W/m}^2$ in CE and $+ 1.0 \text{ W/m}^2$ in NE,
271 Fig. 3c), afforestation in central and northern Europe led to a mean local surface cooling of -0.5 K and
272 -0.3 K, respectively. The maximum mean local cooling effect in central Europe was about -2.6 K, and -
273 1.6 K in northern Europe.

274 In contrast to the local effects of afforestation in winter, local temperature changes in summer are in
275 fact statistically significant, as calculated by a Wilcoxon-Rank-Sum-Test at a 95 % level. In northern
276 Europe, 22 % of the afforested areas show statistically significant temperature changes. In central
277 Europe, 34 % of the temperature changes with afforestation are statistically significant, in southern

278 Europe as much as 63 %. However, this also means that for 78 % of the afforested areas in northern
279 Europe, for 66 % in central Europe, and for 37 % in southern Europe simulated temperature changes
280 are not significant. Although for these non-significant regions afforestation has the same physical
281 effects and the same process chain is simulated as for the significant areas, random causes for the
282 temperature changes in the non-significant regions cannot be excluded.

283

284 **3.2. Non-local effects**

285 **3.2.1 Winter**

286 The non-local effects of afforestation in Europe on the mean climate conditions in winter are now
287 investigated (Fig. 5). In the period 1986-2015, local afforestation led to a slight warming in Scandinavia,
288 central Europe and parts of southern Europe, more precisely Italy and the Balkan region (Fig. 5a). The
289 locally increased evapotranspiration rates with afforestation (Fig. 3b) enhanced the moisture content
290 in the atmosphere, with the consequence that the mean cloud cover in winter was slightly increased
291 over these regions (Fig. 5b). From the perspective of the surface energy balance, the effects of clouds
292 are stronger in winter on the outgoing long-wave radiation than on the incoming short-wave radiation,
293 due to generally short sunshine duration. Therefore, the net short-wave radiation was just slightly
294 reduced in these regions (Fig. 5c), while the reduction in the net long-wave radiation was stronger (Fig.
295 5d). This reduction in outgoing long-wave radiation led consequently to a decreased nocturnal cooling
296 and thus, to higher mean surface temperatures in Scandinavia, central Europe and parts of southern
297 Europe for the period 1986-2015. The mean non-local warming in these regions was +0.06 K, with a
298 warming less than +0.14 K in 90 % of the area. However, only a small proportion of these non-local
299 temperature changes are statistically significant. Only in southern Europe, the non-local warming with
300 afforestation was significant at 15 % of the affected area. For the other regions, no statistically
301 significant temperature changes were simulated. Thus, random causes for the differences between
302 AFF and REF cannot be excluded.

303 The local temperature changes with afforestation are clearly larger than the surrounding non-local
304 changes, as **can be seen** in Figure 5. In addition, the local temperature changes show often an opposite
305 sign and thus, are detached from the large-scale temperature patterns.

306

307 **3.2.2 Summer**

308 As already described for the winter season, the locally increased evapotranspiration rates in afforested
309 areas (Fig. 3b) enhanced also the atmospheric moisture content in summer under the dominant west-
310 wind circulation. The mean downwind cloud cover (Fig. 6b) and precipitation sums (Fig. 6c) were
311 consequently slightly increased over large parts of central and eastern Europe in the period 1986-2015.
312 Exceptions were an area north of the Black Sea and parts of north-eastern Europe. In the upwind areas

313 of western Europe, however, no systematic changes with afforestation were simulated for the mean
314 seasonal cloud cover and the mean seasonal precipitation sums.

315 The increased mean precipitation sums in downwind direction slightly enlarged the amount of
316 available water for evapotranspiration in these regions. As a result, the mean seasonal
317 evapotranspiration rates were also enhanced in non-afforested regions of Europe (Fig. 6d), and thus,
318 more radiative energy could be transformed into latent heat instead of heating up the land surface in
319 summer.

320 In addition, the increased mean cloud cover slightly reduced the incoming mean solar radiation in
321 summer (Fig. 6e) and thus, the radiative energy input in the respective regions. Therefore, the local
322 afforestation in Europe led mainly to a slight cooling in the non-afforested areas of central and eastern
323 Europe in summer for the period 1986-2015 (Fig. 6a). The mean non-local cooling effect in these
324 regions was -0.06 K, with a cooling less than -0.13 K in 10 % of the area. Exceptions are the areas north
325 of the Black Sea and parts of north-eastern Europe where the mean cloud cover and the mean
326 precipitation sums were reduced. The mean non-local warming in these areas was +0.05 K, with a
327 warming less than +0.11 K in 90 % of the area. Just like in winter, the non-local temperature changes
328 in summer are not statistically significant, although these non-local effects can be explained by a
329 physically consistent process chain. Therefore, random causes for the temperature changes cannot be
330 excluded. Furthermore, the local temperature changes are again **pronounced more strongly** than non-
331 local changes and detached from the large-scale temperature pattern.

332

333 **3.3. Extremes**

334 **3.3.1. Temperature extremes**

335 The non-local effects of afforestation on heat extremes (Fig. 7a) showed the same spatial patterns as
336 for the mean temperature effects in summer (Fig. 6a). The daily maximum temperatures during heat
337 extremes were slightly reduced over large parts of Europe, but slightly increased in an area north of
338 the Black Sea and in parts of north-eastern Europe. However, the regional warming in these areas is
339 **pronounced more strongly** than for the mean conditions in summer.

340 During heat periods, the surface energy budget strongly depends on the available amount of soil water
341 for evapotranspiration. A reduction of the soil water availability has the consequence that less solar
342 radiation can be transformed into latent heat and more energy is used to heat up the surface. The
343 reduction of the mean seasonal precipitation sums north of the Black Sea and in north-eastern Europe
344 during summer (Fig. 6c), leads in these regions to such a soil water limitation. The heat period
345 intensities were therefore enhanced in these areas.

346 In the regions in which afforestation had a non-local cooling effect, the daily maximum temperatures
347 during heat extremes were reduced in mean by -0.1 K, with no cooling below -0.2 K in 90 % of the area.

348 Comparable temperature effects were simulated for the regions in which afforestation had a non-local
349 warming effect. North of the Black Sea and in parts of north-eastern Europe, heat extremes were in
350 mean intensified by +0.1 K with a 90th percentile of +0.2 K. The non-local effects of afforestation on
351 heat extreme intensities were consequently low.

352 The local effects of afforestation on the daily maximum temperatures during heat extremes were
353 partly stronger. All over Europe, the intensities of heat extremes were locally reduced with
354 afforestation. Although the mean local cooling effect was with -0.2 K comparable to the non-local
355 effect, at some locations in southern Europe, temperature reductions as strong as -1.9 K were
356 simulated during heat extremes.

357 Fig. 7b shows the effects of afforestation on cold extreme intensities in Europe for the period 1986-
358 2015. In general, afforestation had the same spatial effects on cold extreme intensities as on the mean
359 surface temperatures in winter (Fig. 5a). In Scandinavia, central Europe and parts of southern Europe
360 (Italy and the Balkan region) cold extremes were reduced, while they were slightly increased in eastern
361 Europe. However, the warming effect of afforestation on cold extreme intensities in Scandinavia,
362 central Europe and southern Europe was more pronounced than the changes in the mean temperature
363 conditions. Although the mean non-local warming was with +0.1 K rather small, maximum warming
364 effects of up to +0.8 K were simulated in these regions.

365 Furthermore, the local effects of afforestation on the mean cold extreme temperatures were
366 intensified. Particularly, the intensification of the local winter cooling in southern Europe is clearly
367 evident during cold extremes. On average, the local daily minimum temperatures were reduced by -
368 0.3 K in this region, while 10 % of the local temperature reduction were even larger than -0.8 K. Thus,
369 local temperature responses had an opposite sign and were detached from the large-scale
370 temperature pattern in southern Europe (Fig. 7b).

371

372 **3.3.2. Precipitation extremes**

373 In summer (S1) as well as in winter (S2), the number of small and moderate precipitation intensities
374 was just slightly increased with afforestation. As shown in Fig. 3, evapotranspiration rates were locally
375 increased with afforestation throughout the year all over Europe and particularly in central Europe.
376 The atmospheric moisture content in Europe was consequently increased and downwind precipitation
377 events became slightly more extensive. However, these increased evapotranspiration rates with
378 afforestation did not affect the number and intensity of extreme precipitation events themselves. For
379 precipitation events larger than 10 mm/day, no significant changes between AFF and REF were
380 simulated over the simulated 30 years, indicating that the contribution of the slightly increased
381 evapotranspiration rates with afforestation to the total precipitated water amount is negligible for
382 such strong events.

383

384 **3.4. Variability**

385 The effects of afforestation in Europe on the interannual climate variability in winter and summer for
386 the local and the non-local scales are shown in Figure 8. On average, afforestation did not change the
387 interannual climate variability in Europe within the period 1986-2015. In both seasons, the mean
388 change in the standard deviation was almost zero, both for the local and the non-local effects.
389 However, a wider range of interannual variability were simulated for both, the summer and the winter
390 season. On the local scale, the spread in variability is higher in summer than in winter. But in both
391 cases, positive as well as negative variability changes with afforestation are evenly distributed and do
392 not show any consistent spatial patterns. Thus, interannual variability changes with afforestation are
393 balanced on the local scale, indicating on random effects caused by the natural climate variability. On
394 the non-local scale, the changes in the interannual variability are almost negligible. Therefore,
395 afforestation did not have systematic effects on the interannual climate variability in Europe in our
396 experiments.

397

398 **4. Discussion**

399 The results of our study reflect the well-known effects of afforestation on the surface temperatures
400 (e.g. Bonan et al., 2008), which are already documented in several measurements (e.g. Li et al., 2015;
401 Duveiller et al., 2018) and modeling studies (e.g. Strandberg & Kjellström, 2019; Davin et al., 2020). On
402 the local scale, European afforestation led to a slight warming of the surface temperatures in winter
403 within the period 1986-2015, with the strongest warming effect in central Europe (Fig. 4a). However,
404 statistically significant local effects of afforestation could only be simulated in summer, where
405 afforestation resulted in a slight local cooling of the surface temperatures, with the strongest cooling
406 effect in southern Europe (Fig. 4b). **These general effects of afforestation on the surface temperatures
407 in summer seem to be independent of the afforested area, as shown by the results of coordinated
408 model intercomparison studies with idealized afforestation scenarios. For instance, Davin et al., (2020)
409 and Breil et al., (2020) show that afforestation would have the same local temperature effects if the
410 whole European continent would be afforested.**

411 In contrast, the small local warming effect in winter is quite astonishing, since it is generally assumed
412 that afforestation is associated with a pronounced warming in the mid-latitudes in boreal winter, as
413 for example shown by Lejeune et al., (2017) for North America. **Using Land-Use and Climate,
414 Identification of Robust Impacts (LUCID) models and Phase 5 of the Coupled Model Intercomparison
415 Project (CMIP5) models, Lejeune et al., (2017) provided evidence that the snow-masking effect of
416 forests (e.g. Essery, 2013) is clearly pronounced in North America. In combination with slightly
417 increased evapotranspiration rates, winter temperatures of forests are about 0.3 K (LUCID) and 0.4 K**

418 (CMIP5) higher than those of other vegetation forms. However, the snow-masking effect is less
419 pronounced in Europe than in North America, as shown by Asselin et al., (2022) within the framework
420 of an idealized afforestation experiment for Europe and North America. They could show that snow-
421 masking reduces the surface albedo on both continents in a similar way, but the reduced surface
422 albedo effect on the surface temperatures is in North America much stronger than in Europe. For the
423 same latitude, European climate is warmer than the climate in North America, and snow cover in
424 winter is consequently restricted only to higher latitudes, notably central and northern Europe. There,
425 insolation is low in winter and thus, the albedo effect on surface temperatures is small. The same
426 conclusions were drawn by Strandberg & Kjellström, (2019) from regional climate simulations with an
427 idealized afforestation scenario for Europe.

428 In southern Europe, where insolation is higher, snow cover plays a minor role for the surface energy
429 balance. Surface temperatures are typically higher than for central and northern Europe, and
430 therefore, buoyancy is generally stronger in this region. In combination with the higher surface
431 roughness of forests and the associated increased wind shear, afforested areas in southern Europe are
432 consequently able to transform this increased energy input from solar radiation efficiently into
433 turbulent heat and release the energy into the atmosphere (e.g. Breil et al., 2020), counteracting the
434 increased solar radiation. Thus, afforestation did not have a warming effect in southern Europe in
435 winter (Fig. 4). These described general effects of afforestation on the different components of the
436 surface energy balance are intensified in summer and also take place in central and northern Europe
437 (Fig. 3; Breil et al., 2020). A general reduction of the surface albedo, an increased release of turbulent
438 energy into the atmosphere and a resulting local cooling in summer are also described by Burakowski
439 et al., (2018) for North America. This indicates that the results of this study may be representative for
440 afforestation in the mid-latitudes and transferable to other regions.

441 Beyond these local effects, afforestation affects the climate conditions in Europe also on the non-local
442 scale (Fig. 5 and Fig. 6). As already demonstrated by Meier et al., (2021), afforestation can increase
443 downwind cloud cover and precipitation sums in Europe by increased evapotranspiration rates and
444 thus, a higher moisture content in the atmosphere. These findings are confirmed by the results of this
445 study (Fig. 6b-d). Although the non-local effects of afforestation can be explained by a physically
446 consistent process chain, simulated non-local temperature changes are statistically not significant in
447 Europe.

448 However, a missing significance does not necessarily mean that there is no causal relationship
449 (Wasserstein & Lazar, 2016) between afforestation and the simulated non-local temperature changes.
450 On the contrary, the traceability of the complete physical process chain is, from our point of view, a
451 strong indicator that the non-local afforestation effects are not random. Particularly downwind
452 processes are spatially and temporally highly variable. Thus, locally induced changes in the

453 atmospheric moisture conditions do not always lead to precipitation and cloud cover at the same
454 downwind locations (Perugini et al., 2017). This high spatial and temporal variability, has the
455 consequence that the mean downwind effects are small and difficult to detect, resulting in not
456 significant temperature changes. Nevertheless, during extreme events, like heat periods in summer or
457 cold spells in winter, the described effects of afforestation on the local and the non-local surface
458 energy and water balance are pronounced more strongly than for the mean climate conditions, so that
459 afforestation had a notable impact on the characteristics of these extremes within the period 1986-
460 2015 (Fig. 7, Breil et al., 2023b).

461 However, the presented work is a modeling study and therefore associated with certain modeling
462 uncertainties. Even though CCLM-VEG3D is able to properly reproduce the observed regional climate
463 conditions in Europe during the simulated 30 years (Fig. 2), the effects of afforestation on the surface
464 temperatures may locally differ from measurement studies (e.g. Li, et al., 2015; Duveiller et al., 2018).
465 These differences to observations might result from the fact that in CCLM-VEG3D only the dominant
466 land use class is considered within a model grid box. This means that the local effects of afforestation
467 on the surface temperatures are overestimated at some places, and underestimated at other places.
468 However, the total afforested area in CCLM-VEG3D has with 1,7 % of the European continent nearly
469 the same extent as the real one with 1.1 % (Hoffman et al., 2022). The simulated total effects of
470 afforestation on the regional surface energy balance in Europe are therefore reasonable, and the
471 applied modeling approach is suitable to analyze the general impact of afforestation on the European
472 climate for the period 1986-2015. Nonetheless, regional variations in the described local and non-local
473 process chains have to be acknowledged.

474 In addition, the results of this study are only valid for evergreen needleleaved trees and deciduous
475 broadleaved trees that are characteristic for the mid-latitudes. Other tree species, like for example
476 evergreen broadleaved trees or deciduous needleleaved trees can of course have other effects on the
477 local surface energy balance and consequently induce other remote effects. The described
478 afforestation effects in this study could therefore be both, stronger and weaker.

479 On the other hand, the advantage of an idealized modeling study like this is that the effects of
480 afforestation on the surface energy balance can be locally isolated and comprehensively analyzed, by
481 performing and comparing simulations with and without afforestation. This is not possible in
482 observation based studies. Thus, the analyzed effects of afforestation on the surface energy balance
483 are in such measurement studies potentially superimposed by other processes, which are not easy to
484 separate from each other.

485 In conclusion, it is noticeable that the temperature changes with afforestation appear to be rather
486 small in Europe. However, in comparison to the mean temperature changes during the investigation
487 period 1986-2015, the impact of afforestation on the climate change signal is considerable. While the

488 mean temperatures in winter rose about 1.7 K in Europe during the simulated 30 years (Twardosz et
489 al., 2021), mean summer temperatures between 1986-2015 were 1.3 K warmer compared to pre-
490 industrial levels (Luterbacher et al., 2016). During the last decade of the investigation period, mean
491 annual temperatures were 1.5 K above pre-industrial levels (European Environment Agency, 2017).
492 Thus, the simulated non-local warming of up to 0.1 K in Scandinavia, central Europe and parts of
493 southern Europe in winter, additionally contributed to the general winter warming signal in these
494 regions. On the other hand, the local cooling effect of afforestation of about -0.3 K in northern Europe
495 and about -0.8 K in southern Europe in summer, may have mitigated the general warming trend in
496 summer. That means that without afforestation, the climate change signal would have been much
497 stronger in these regions for the period 1986-2015, especially in summer.

498

499 **5. Conclusions**

500 In this study, we analyzed the general effects of afforestation on the regional climate conditions in
501 Europe for the period 1986-2015, by performing long-term regional climate simulations, with one
502 simulation considering changes in forest cover and another simulation not accounting for changes in
503 forest cover. The comparison of these simulations reveals that afforestation led to a discernible
504 reduction of the mean local surface temperatures all over Europe in summer in the simulated 30 years.
505 In northern and central Europe local surface temperatures were reduced by -0.3 K and -0.5 K,
506 respectively. In southern Europe, this cooling effect is particularly pronounced and a mean local cooling
507 of -0.8 K was simulated. During heat extremes, the local cooling effect of afforestation is intensified.
508 At some locations in Europe, temperature reductions reached values up to -1.9 K. In winter,
509 afforestation did not have a significant local effect, due to a small general impact of the snow masking
510 effect.

511 Beyond these local effects, afforestation had also an impact on the downwind climate conditions. By
512 increasing the local evapotranspiration rates, afforestation led to an increase in the atmospheric
513 moisture content, and thus to a non-locally enhanced cloud cover and precipitation sums in
514 Scandinavia, central Europe and parts of southern Europe. These changes in the atmospheric water
515 cycle resulted in a slight warming of the mean non-local surface temperatures in winter and a slight
516 cooling in these regions in summer. Although these mean non-local temperature changes are not
517 statistically significant, non-local afforestation effects can be consistently explained by non-local
518 changes in the energy and water balance, which had especially during temperature extremes a notable
519 impact on the non-local climate conditions in Europe.

520

521 **Data availability**

522 The applied land use dataset is accessible at the World Data Center for Climate (WDCC) at DKRZ
523 (https://doi.org/10.26050/WDCC/LUC_hist_EU_v1.1). The ERA-5 reanalysis data are obtained from
524 the ECMWF (<https://apps.ecmwf.int/data-catalogues/era5/?class=ea>). The CCLM-VEG3D data is
525 available upon request from the corresponding author.

526

527 **Author contributions**

528 MB designed the study, performed the CCLM-VEG3D simulations and wrote the paper. MB and VKMS
529 analyzed the data and MB prepared the figures. All authors contributed with discussion, interpretation
530 of results and text revisions.

531

532 **Competing interests**

533 The contact author has declared that none of the authors has any competing interests.

534

535 **Financial support**

536 Marcus Breil was supported by the Vector Foundation. Joaquim G. Pinto was supported by the AXA
537 Research Fund.

538

539

540

541

542

543

544

545

546

547

548

549

550

551

552

553

554

555

556

557 **References**

558 Asselin, O., Leduc, M., Paquin, D., Di Luca, A., Winger, K., Bukovsky, M., Music, B., & Giguère, M.: On
559 the Intercontinental Transferability of Regional Climate Model Response to Severe Forestation.
560 *Climate*, 10(10), 138, <https://doi.org/10.3390/cli10100138>, 2022

561
562 Bala, G., Caldeira, K., Wickett, M., Phillips, T. J., Lobell, D. B., Delire, C., & Mirin, A.: Combined climate
563 and carbon-cycle effects of large-scale deforestation. *Proceedings of the National Academy of Sciences*,
564 104(16), 6550-6555, <https://doi.org/10.1073/pnas.0608998104>, 2007.

565
566 Bonan, G. B.: Forests and climate change: forcings, feedbacks, and the climate benefits of forests.
567 *Science*, 320(5882), 1444-1449, [DOI: 10.1126/science.1155121](https://doi.org/10.1126/science.1155121), 2008.

568
569 Breil, M., & Schädler, G.: The reduction of systematic temperature biases in soil moisture-limited
570 regimes by stochastic root depth variations, *Journal of Hydrometeorology*, 22(7), 1897-1911,
571 <https://doi.org/10.1175/JHM-D-20-0265.1>, 2021.

572
573 Breil, M., Rechid, D., Davin, E. L., de Noblet-Ducoudré, N., Katragkou, E., Cardoso, R. M., Hoffmann, P.,
574 Jach, L.L., Soares, P.M.M., Sofiadis, G., Strada, S., Strandberg, G., Tölle, M.H., & Warrach-Sagi, K. (2020).
575 The opposing effects of reforestation and afforestation on the diurnal temperature cycle at the surface
576 and in the lowest atmospheric model level in the European summer. *Journal of Climate*, 33(21), 9159-
577 9179, <https://doi.org/10.1175/JCLI-D-19-0624.1>, 2020.

578
579 Breil, M., Krawczyk, F., and Pinto, J. G.: The response of the regional longwave radiation balance and
580 climate system in Europe to an idealized afforestation experiment, *Earth Syst. Dynam.*, 14, 243–253,
581 <https://doi.org/10.5194/esd-14-243-2023>, 2023a.

582
583 Breil, M., Weber, A., & Pinto, J. G.: The potential of an increased deciduous forest fraction to mitigate
584 the effects of heat extremes in Europe. *Biogeosciences Discussions*, 1-25, accepted, 2023b.

585
586 Bright, R. M., Davin, E., O'Halloran, T., Pongratz, J., Zhao, K., & Cescatti, A.: Local temperature response
587 to land cover and management change driven by non-radiative processes. *Nature Climate Change*,
588 7(4), 296-302, <https://doi.org/10.1038/nclimate3250>, 2017.

589
590 Burakowski, E., Tawfik, A., Ouimette, A., Lepine, L., Novick, K., Ollinger, S., Zarzycki, C., & Bonan, G.:
591 The role of surface roughness, albedo, and Bowen ratio on ecosystem energy balance in the Eastern

592 United States. *Agricultural and Forest Meteorology*, 249, 367-376,
593 <https://doi.org/10.1016/j.agrformet.2017.11.030>, 2018.

594

595 Davin, E. L., Rechid, D., Breil, M., Cardoso, R. M., Coppola, E., Hoffmann, P., Jach, L. L., Katragkou, E.,
596 de Noblet-Ducoudré, N., Radtke, K., Raffa, M., Soares, P. M. M., Sofiadis, G., Strada, S., Strandberg, G.,
597 Tölle, M. H., Warrach-Sagi, K., & Wulfmeyer, V.: Biogeophysical impacts of forestation in Europe: first
598 results from the LUCAS (Land Use and Climate Across Scales) regional climate model intercomparison.
599 *Earth System Dynamics*, 11(1), 183-200, <https://doi.org/10.5194/esd-11-183-2020>, 2020.

600

601 Duveiller, G., Hooker, J., & Cescatti, A.: The mark of vegetation change on Earth's surface energy
602 balance. *Nature communications*, 9(1), 679, <https://doi.org/10.1038/s41467-017-02810-8>, 2018.

603

604 European Space Agency: Land Cover CCI Product User Guide Version 2, Tech. rep., European Space
605 Agency, maps.elie.ucl.ac.be/CCI/viewer/download/645ESACCI-LC-Ph2-PUGv2_2.0.pdf, 2017.

606

607 European Environment Agency: Climate change, impacts and vulnerability in Europe 2016: an
608 indicator-based report, Publications Office, <https://doi.org/10.2800/534806>, 2017.

609

610 Essery, R.: Large-scale simulations of snow albedo masking by forests. *Geophysical Research Letters*,
611 40(20), 5521-5525, <https://doi.org/10.1002/grl.51008>, 2013.

612

613 Gulev, S.K., P.W. Thorne, J. Ahn, F.J. Dentener, C.M. Domingues, S. Gerland, D. Gong, D.S. Kaufman,
614 H.C. Nnamchi, J. Quaas, J.A. Rivera, S. Sathyendranath, S.L. Smith, B. Trewin, K. von Schuckmann, and
615 R.S. Vose: Changing State of the Climate System. In *Climate Change 2021: The Physical Science Basis*.
616 Contribution of Working Group I to the Sixth Assessment Report of the Intergovernmental Panel on
617 Climate Change [Masson-Delmotte, V., P. Zhai, A. Pirani, S.L. Connors, C. Péan, S. Berger, N. Caud, Y.
618 Chen, L. Goldfarb, M.I. Gomis, M. Huang, K. Leitzell, E. Lonnoy, J.B.R. Matthews, T.K. Maycock, T.
619 Waterfield, O. Yelekçi, R. Yu, and B. Zhou (eds.)]. Cambridge University Press, Cambridge, United
620 Kingdom and New York, NY, USA, pp. 287–422, [doi:10.1017/9781009157896.004](https://doi.org/10.1017/9781009157896.004), 2021.

621

622 Harper, A. B., Powell, T., Cox, P. M., House, J., Huntingford, C., Lenton, T. M., Sitch, S., Burke, E.,
623 Chadburn, S. E., Collins, W. J., Comyn-Platt, E., Daioglou, V., Doelman, J. C., Hayman, G., Robertson, E.,
624 van Vuuren, D., Wiltshire, A., Webber, C. P., Bastos, A., Boysen, L., Ciais, P., Devaraju, N., Jain, A. K.,
625 Krause, A., Poulter, B., & Shu, S.: Land-use emissions play a critical role in land-based mitigation for

626 Paris climate targets. *Nature communications*, 9(1), 1-13, <https://doi.org/10.1038/s41467-018-05340->
627 [z](https://doi.org/10.1038/s41467-018-05340-z), 2018.

628

629 Hersbach, H., Bell, B., Berrisford, P., Hirahara, S., Horanyi, A., Muñoz-Sabater, J., Nicolas, J., Peubey, C.,
630 Radu, R., Schepers, D., Simmons, A., Soci, C., Abdalla, S., Abellan, X., Balsamo, G., Bechtold, P., Biavati,
631 G., Bidlot, J., Bonavita, M., de Chiara, G., Dahlgren, P., Dee, D., Diamantakis, M., Dragani, R., Flemming,
632 J., Forbes, R., Fuentes, M., Geer, A., Haimberger, L., Healy, S., Hogan, R. J., Holm, E., Janiskova, M.,
633 Keeley, S., Laloyaux, P., Lopez, P., Lupu, C., Radnoti, G., de Rosnay, P., Rozum, I., Vamborg, F., Villaume,
634 S., Thepaut, J.-N.: The ERA5 global reanalysis. *Quarterly Journal of the Royal Meteorological Society*,
635 146 (730), 1999–2049, <https://doi.org/10.1002/qj.3803>, 2020.

636

637 Hoffmann, P., Reinhart, V., Rechid, D., de Noblet-Ducoudré, N., Davin, E. L., Asmus, C., Bechtel, B.,
638 Böhner, J., Katragkou, E., & Luyssaert, S.: High-resolution land use and land cover dataset for regional
639 climate modelling: Historical and future changes in Europe. *Earth System Science Data Discussions*,
640 <https://doi.org/10.5194/essd-2022-431>, 2022.

641

642 Hurtt, G. C., Chini, L., Sahajpal, R., Frohling, S., Bodirsky, B. L., Calvin, K., Doelman, J. C., Fisk, J., Fujimori,
643 S., Klein Goldewijk, K., Hasegawa, T., Havlik, P., Heinemann, A., Humpenöder, F., Jungclaus, J., Kaplan,
644 J. O., Kennedy, J., Krisztin, T., Lawrence, D., Lawrence, P., Ma, L., Mertz, O., Pongratz, J., Popp, A.,
645 Poulter, B., Riahi, K., Shevliakova, E., Stehfest, E., Thornton, P., Tubiello, F. N., van Vuuren, D. P., and
646 Zhang, X.: Harmonization of global land use change and management for the period 850–2100 (LUH2)
647 for CMIP6, *Geoscientific Model Development*, 13, 5425–5464, <https://doi.org/10.5194/gmd-13-5425->
648 [2020](https://doi.org/10.5194/gmd-13-5425-2020), 2020.

649

650 Jacob, D., Petersen, J., Eggert, B., Alias, A., Christensen, O. B., Bouwer, L. M., Braun, A., Colette, A.,
651 Deque, M., Georgievski, G., Georgopoulou, E., Gobiet, A., Menut, L., Nikulin, G., Haensler, A.,
652 Hempelmann, N., Jones, C., Keuler, K., Kovats, S., Kröner, N., Kotlarski, S., Kriegsmann, A., Martin, E.,
653 van Meijgaard, E., Moseley, C., Pfeifer, S., Preuschmann, S., Radermacher, C., Radtke, K., Rechid, D.,
654 Rounsevell, M., Samuelsson, P., Somot, S., Soussana J.-F., Teichmann, C., Valentini, R., Vautard, R.,
655 Weber, B., & Yiou, P.: EURO-CORDEX: new high-resolution climate change projections for European
656 impact research. *Regional environmental change*, 14(2), 563-578, <https://doi.org/10.1007/s10113->
657 [013-0499-2](https://doi.org/10.1007/s10113-013-0499-2), 2014.

658

659 Kotlarski, S., Keuler, K., Christensen, O. B., Colette, A., Déqué, M., Gobiet, A., Goergen, K., Jacob, D.,
660 Lüthi, D., van Meijgaard, E., Nikulin, G., Schär, C., Teichmann, C., Vautard, R., Warrach-Sagi, K., &

661 Wulfmeyer, V.: Regional climate modeling on European scales: a joint standard evaluation of the
662 EURO-CORDEX RCM ensemble. *Geoscientific Model Development*, 7(4), 1297-1333,
663 <https://doi.org/10.5194/gmd-7-1297-2014>, 2014.

664

665 Lawrence, D., & Vandecar, K.: Effects of tropical deforestation on climate and agriculture. *Nature*
666 *climate change*, 5(1), 27-36, <https://doi.org/10.1038/nclimate2430>, 2015.

667

668 Lee, X., Goulden, M. L., Hollinger, D. Y., Barr, A., Black, T. A., Bohrer, G., Bracho, R., Drake, B., Goldstein,
669 A., Gu, L., Katul, G., Kolb, T., Law, B. E., Margolis, H., Meyers, T., Monson, R., Munger, W., Oren, R.,
670 Paw, K. T. U., Richardson, A. D., Schmid, H. P., Staebler, R., Wofsy, S., & Zhao, L.: Observed increase in
671 local cooling effect of deforestation at higher latitudes. *Nature*, 479(7373), 384-387,
672 <https://doi.org/10.1038/nature10588>, 2011.

673

674 Leuschner, C., Hertel, D., Coners, H., & Büttner, V.: Root competition between beech and oak: a
675 hypothesis. *Oecologia*, 126(2), 276-284, <https://doi.org/10.1007/s004420000507>, 2001.

676

677 Lejeune, Q., Seneviratne, S. I., & Davin, E. L.: Historical land-cover change impacts on climate:
678 Comparative assessment of LUCID and CMIP5 multimodel experiments. *Journal of Climate*, 30(4),
679 1439-1459, <https://doi.org/10.1175/JCLI-D-16-0213.1>, 2017.

680

681 Li, Y., Zhao, M., Motesharrei, S., Mu, Q., Kalnay, E., & Li, S.: Local cooling and warming effects of forests
682 based on satellite observations. *Nature communications*, 6(1), 6603,
683 <https://doi.org/10.1038/ncomms7603>, 2015.

684

685 Luterbacher, J., Werner, J. P., Smerdon, J. E., Fernández-Donado, L., González-Rouco, F. J., Barriopedro,
686 D., Ljungqvist, F. C., Büntgen, U., Zorita, E., Wagner, S., Esper, J., McCarroll, D., Toreti, A., Frank, D.,
687 Jungclaus, J. H., Barriendos, M., Bertolin, C., Bothe, O., Brázdil, R., Camuffo, D., Dobrovolný, P., Gagen,
688 M., García-Bustamante, E., Ge, Q., Gómez-Navarro, J. J., Guiot, J., Hao, Z., Hegerl, G. C., Holmgren, K.,
689 Klimenko, V. V., Martín-Chivelet, J., Pfister, C., Roberts, N., Schindler, A., Schurer, A., Solomina, O., von
690 Gunten, L., Wahl, E., Wanner, H., Wetter, O., Xoplaki, E., Yuan, N., Zanchettin, D., Zhang, H., & Zerefos,
691 C.: European summer temperatures since Roman times. *Environmental research letters*, 11(2), 024001,
692 [10.1088/1748-9326/11/2/024001](https://doi.org/10.1088/1748-9326/11/2/024001), 2016.

693

694 Luysaert, S., Ciais, P., Piao, S. L., Schulze, E. D., Jung, M., Zaehle, S., Schelhaas, M. J., Reichstein, M.,
695 Churkina, G., Papale, D., Abril, G., Beer, C., Grace, J., Loustau, D., Matteucci, G., Magnani, F., Nabuurs,

696 G. J., Verbeeck, H., Sulkava, M., van der Werf, G. R., Janssens, I. A., & members of the CARBOEUROPE-
697 IP SYNTHESIS TEAM: The European carbon balance. Part 3: forests. *Global Change Biology*, 16(5), 1429-
698 1450, <https://doi.org/10.1111/j.1365-2486.2009.02056.x>, 2010.

699

700 Meier, R., Schwaab, J., Seneviratne, S. I., Sprenger, M., Lewis, E., & Davin, E. L.: Empirical estimate of
701 forestation-induced precipitation changes in Europe. *Nature geoscience*, 14(7), 473-478,
702 <https://doi.org/10.1038/s41561-021-00773-6>, 2021.

703

704 Muñoz-Sabater, J., Dutra, E., Agustí-Panareda, A., Albergel, C., Arduini, G., Balsamo, G., Boussetta, S.,
705 Choulga, M., Harrigan, S., Hersbach, H., Martens, B., Miralles, D. G., Piles, M., Rodríguez-Fernández, N.
706 J., Zsoter, E., Buontempo, C., and Thépaut, J.-N.: ERA5-Land: a state-of-the-art global reanalysis dataset
707 for land applications, *Earth Syst. Sci. Data*, 13, 4349–4383, [https://doi.org/10.5194/essd-13-4349-](https://doi.org/10.5194/essd-13-4349-2021)
708 [2021](https://doi.org/10.5194/essd-13-4349-2021), 2021.

709

710 Pan, Y., Birdsey, R. A., Fang, J., Houghton, R., Kauppi, P. E., Kurz, W. A., .Phillips, O. L., Shvidenko, A.,
711 Lewis, S. L., Canadell, J. G., Ciais, P., Jackson, R. B., Pacala, S. W., McGuire, A. D., Paio, S., Rautiainen,
712 A., Sitch, S., & Hayes, D.: A large and persistent carbon sink in the world's forests. *Science*, 333(6045),
713 988-993, [DOI: 10.1126/science.1201609](https://doi.org/10.1126/science.1201609), 2011.

714

715 Perugini, L., Caporaso, L., Marconi, S., Cescatti, A., Quesada, B., de Noblet-Ducoudré, N., House, J. I., &
716 Arneth, A.: Biophysical effects on temperature and precipitation due to land cover change.
717 *Environmental Research Letters*, 12(5), 053002, [10.1088/1748-9326/aa6b3f](https://doi.org/10.1088/1748-9326/aa6b3f), 2017.

718

719 Pielke Sr, R. A., Pitman, A., Niyogi, D., Mahmood, R., McAlpine, C., Hossain, F., Goldewijk, K. K., Nair,
720 U., Betts, R., Fall, S., Reichstein, M., Kabat, P., & de Noblet, N.: Land use/land cover changes and
721 climate: modeling analysis and observational evidence. *Wiley Interdisciplinary Reviews: Climate*
722 *Change*, 2(6), 828-850, [doi: 10.1002/wcc.144](https://doi.org/10.1002/wcc.144), 2011.

723

724 Rockel, B., Will, A., & Hense, A.: The Regional Climate Model COSMO-CLM (CCLM). *Meteorologische*
725 *Zeitschrift*, 17 (4), 347–348, <https://doi.org/10.1127/0941-2948/2008/0309>, 2008.

726

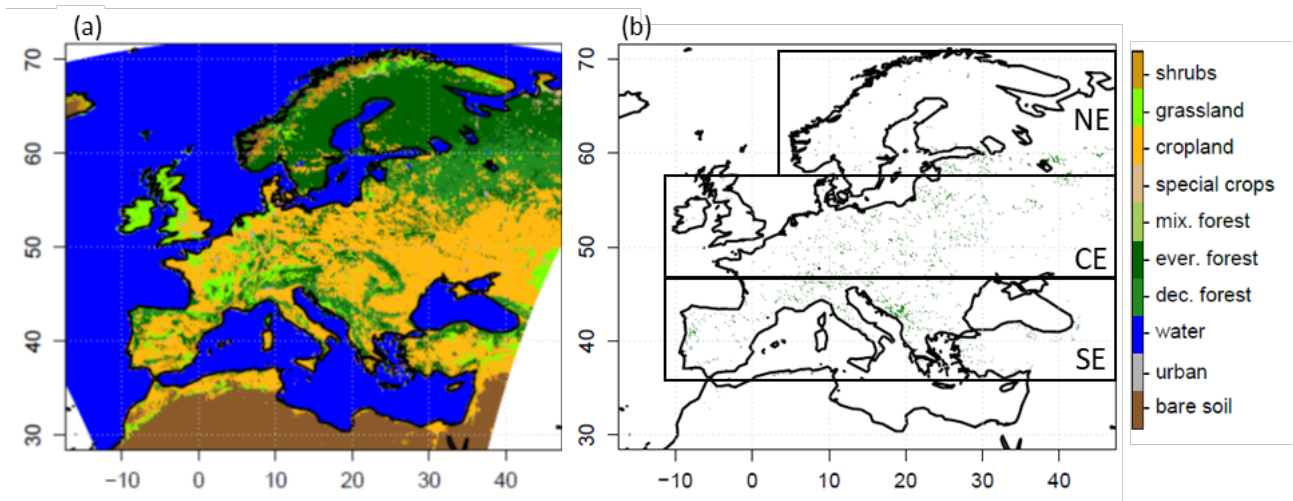
727 Roe, S., Streck, C., Obersteiner, M., Frank, S., Griscom, B., Drouet, L., Fricko, O., Gusti, M., Harris, N.,
728 Hasegawa, T., Hausfather, Z., Havlik, P., House, J., Nabuurs, G.-J., Popp, A., Sanz Sanchez, M. J.,
729 Sanderman, J., Smit, P., Stehfest, E., & Lawrence, D.: Contribution of the land sector to a 1.5 C world.
730 *Nature Climate Change*, 9(11), 817-828, <https://doi.org/10.1038/s41558-019-0591-9>, 2019.

731
732 Seneviratne, S. I., Corti, T., Davin, E. L., Hirschi, M., Jaeger, E. B., Lehner, I., Orlowsky, B., & Teuling, A.
733 J.: Investigating soil moisture–climate interactions in a changing climate: A review. *Earth-Science*
734 *Reviews*, 99(3-4), 125-161, <https://doi.org/10.1016/j.earscirev.2010.02.004>, 2010.
735
736 Sonntag, S., Pongratz, J., Reick, C. H., & Schmidt, H.: Reforestation in a high-CO2 world—Higher
737 mitigation potential than expected, lower adaptation potential than hoped for. *Geophysical Research*
738 *Letters*, 43(12), 6546-6553, <https://doi.org/10.1002/2016GL068824>, 2016.
739
740 Strandberg, G., & Kjellström, E.: Climate impacts from afforestation and deforestation in Europe. *Earth*
741 *Interactions*, 23(1), 1-27, <https://doi.org/10.1175/EI-D-17-0033.1>, 2019.
742
743 Twardosz, R., Walanus, A., & Guzik, I.: Warming in Europe: Recent trends in annual and seasonal
744 temperatures. *Pure and Applied Geophysics*, 178(10), 4021-4032, [https://doi.org/10.1007/s00024-](https://doi.org/10.1007/s00024-021-02860-6)
745 [021-02860-6](https://doi.org/10.1007/s00024-021-02860-6), 2021.
746
747 Wasserstein, R. L., & Lazar, N. A.: The ASA statement on p-values: context, process, and purpose. *The*
748 *American Statistician*, 70(2), 129-133, <https://doi.org/10.1080/00031305.2016.1154108>, 2016.
749
750 Zeppetello, L. R. V., Parsons, L. A., Spector, J. T., Naylor, R. L., Battisti, D. S., Masuda, Y. J., & Wolff, N.
751 H.: Large scale tropical deforestation drives extreme warming. *Environmental Research Letters*, 15(8),
752 084012, [10.1088/1748-9326/ab96d2](https://doi.org/10.1088/1748-9326/ab96d2), 2020.
753
754 Zhang, L., Dawes, W. R., & Walker, G. R.: Response of mean annual evapotranspiration to vegetation
755 changes at catchment scale. *Water resources research*, 37(3), 701-708,
756 <https://doi.org/10.1029/2000WR900325>, 2001.
757
758
759
760
761
762
763
764
765

766 Table 1: Maximum parameter values of the surface roughness, leaf area index (LAI), surface albedo,
767 and root depth used in CCLM-VEG3D for deciduous forests, coniferous forests, croplands, and
768 grasslands.

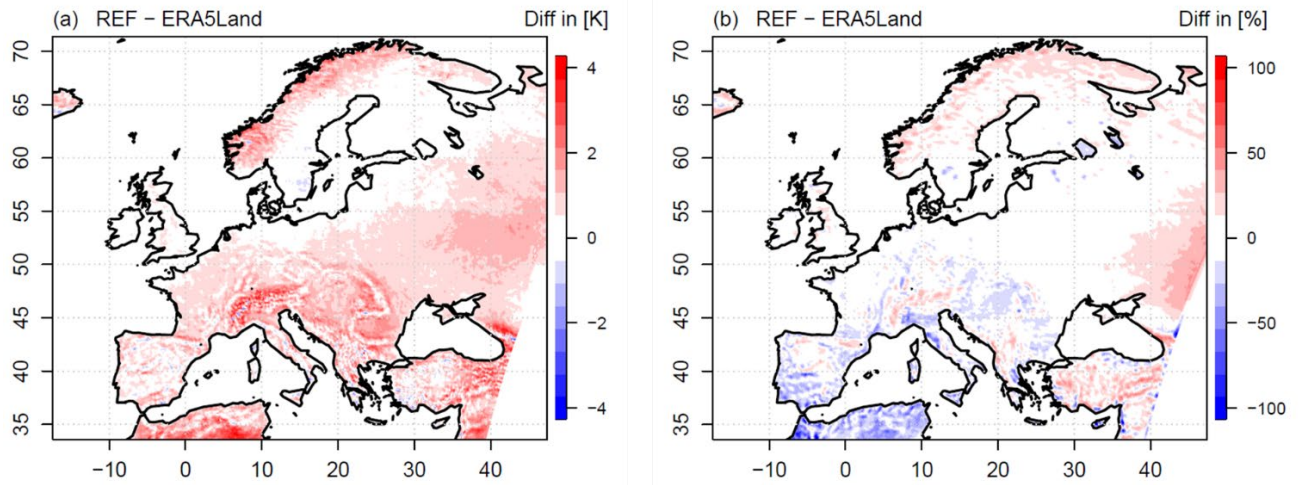
	LAI	root depth (density < 2%)	albedo	surface roughness
deciduous forest	8	2.0 m	0.15	0.8 m
coniferous forest	9	1.0 m	0.11	1.0 m
croplands	3.5	1.0 m	0.2	0.07 m
grasslands	4	0.5 m	0.2	0.03 m

769
770
771
772
773
774
775
776
777
778
779
780
781
782
783
784
785
786
787
788
789
790
791



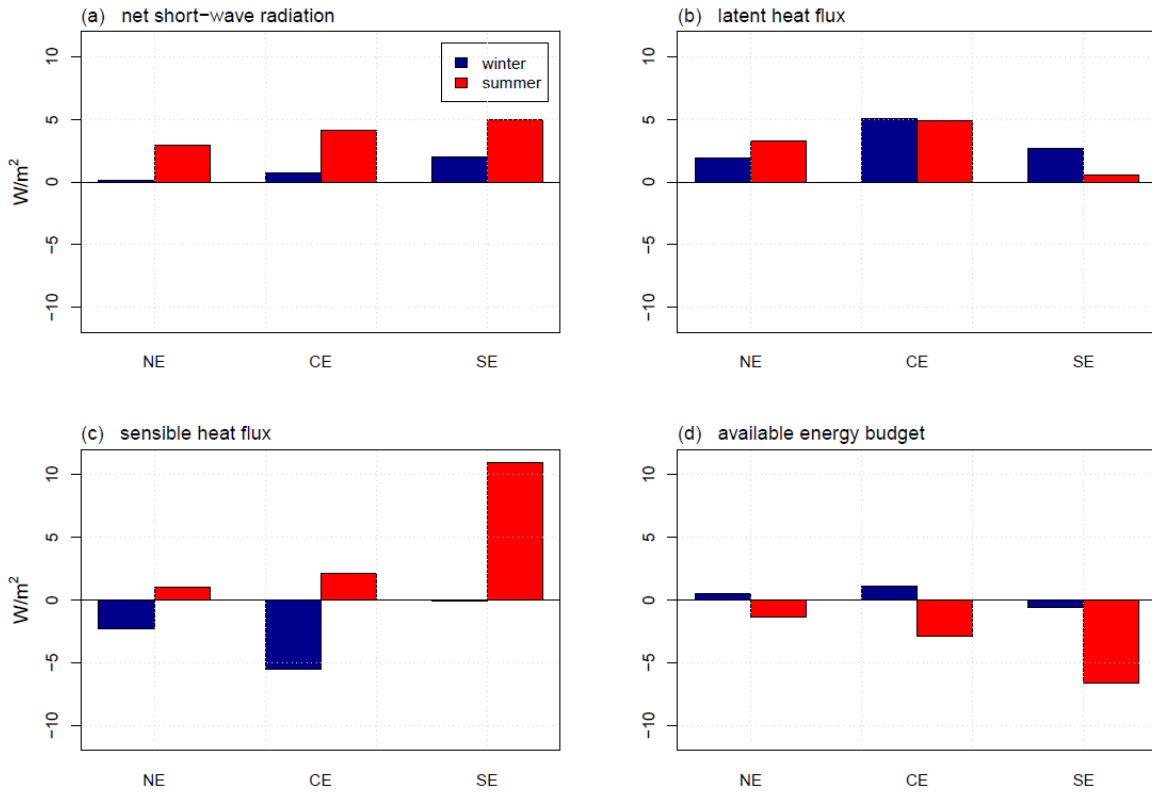
792
 793 Figure 1: (a) CCLM-VEG3D land use classes. (b) grid cells in which afforestation took place between
 794 1986-2015 in the AFF simulation. The black boxes show the locations of the three geographical sub-
 795 regions, northern Europe (NE), central Europe (CE) and southern Europe (SE).

796
 797
 798
 799
 800
 801
 802
 803
 804
 805
 806
 807
 808
 809
 810
 811
 812
 813
 814
 815
 816
 817
 818
 819
 820
 821
 822
 823
 824
 825
 826
 827



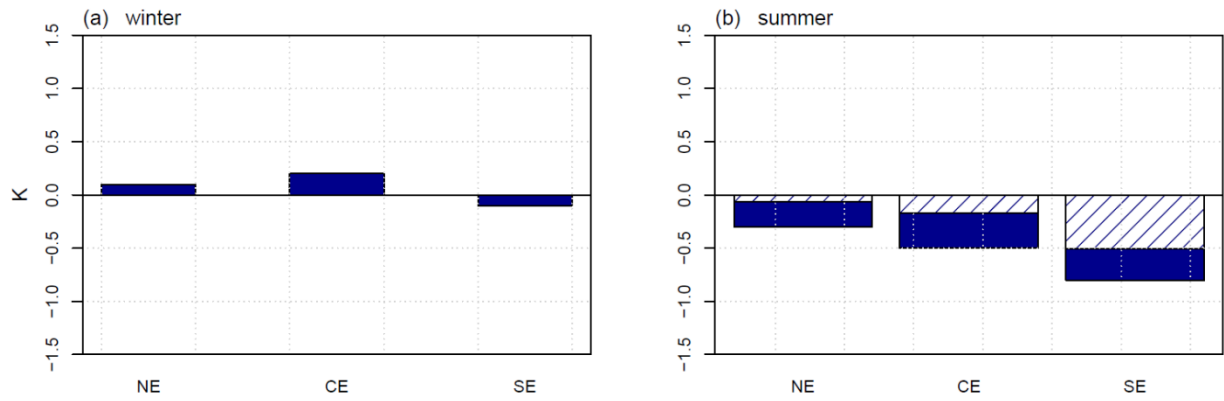
828
 829 Figure 2: Differences in the (a) yearly mean 2 m temperature and (b) the percentage deviation in the
 830 yearly mean total precipitation sums between REF and the ERA5-Land reanalysis for the period 1986-
 831 2015.

832
 833
 834
 835
 836
 837
 838
 839
 840
 841
 842
 843
 844



845
 846 Figure 3: Local effects of afforestation (AFF-REF) on (a) the mean net short-wave radiation (R), (b) the
 847 mean latent heat fluxes (L), (c) the mean sensible heat fluxes (H), and (d) the available energy budget
 848 at the surface (defined as $R - (L+H)$), for the three subregions NE, CE and SE. Local effects in winter are
 849 shown in blue, local effects in summer are shown in red.

850
 851
 852
 853
 854
 855
 856
 857
 858
 859
 860
 861
 862
 863



864

865

866 Figure 4: Local effects of afforestation (AFF-REF) on the mean surface temperature in (a) winter, and

867 (b) summer for the three subregions NE, CE and SE. The fraction of significant local effects in the

868 respective subregions (calculated with a Wilcoxon-Rank-Sum-Test at a 95 % level) are indicated by

869 dashed lines.

870

871

872

873

874

875

876

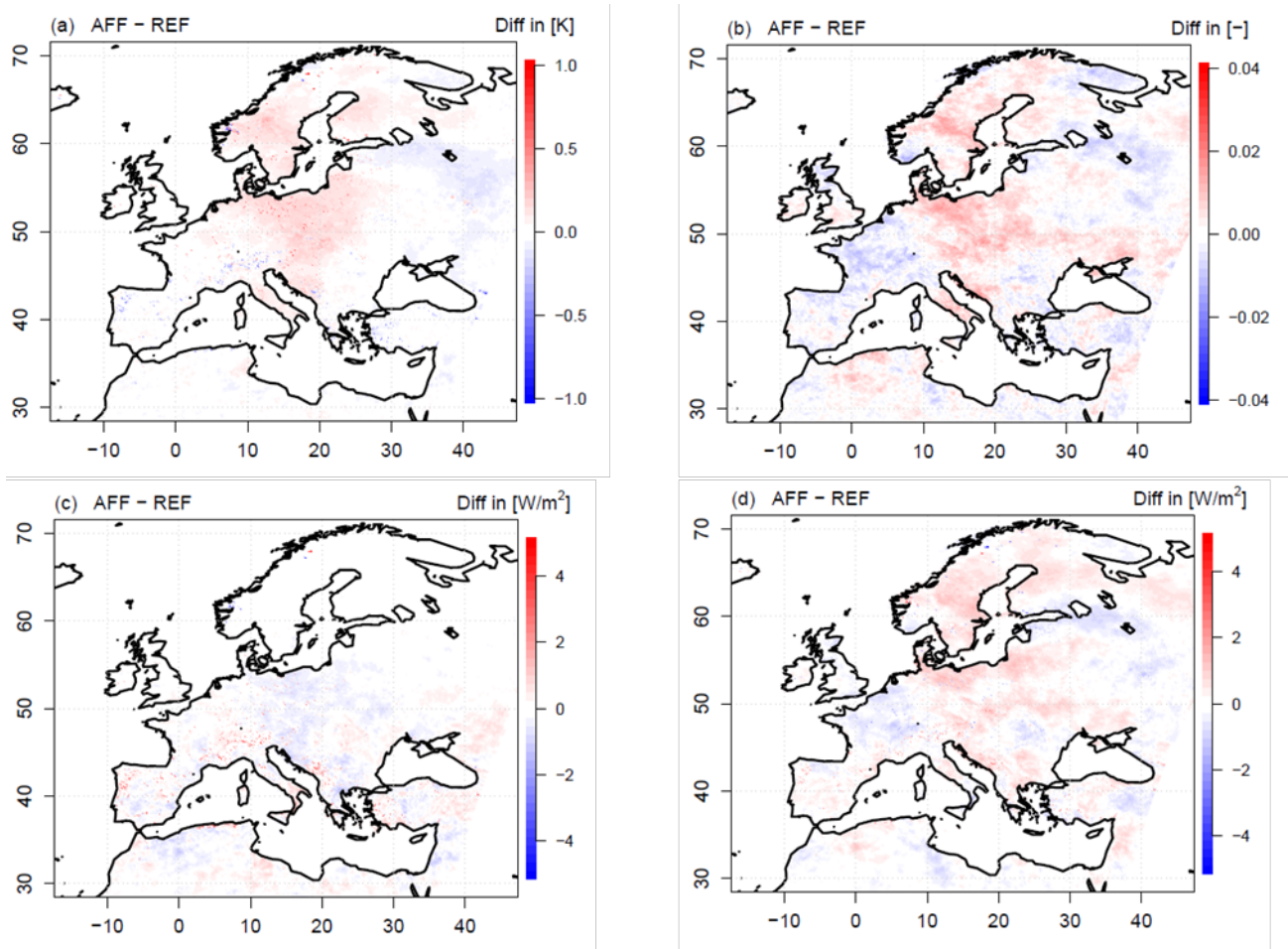
877

878

879

880

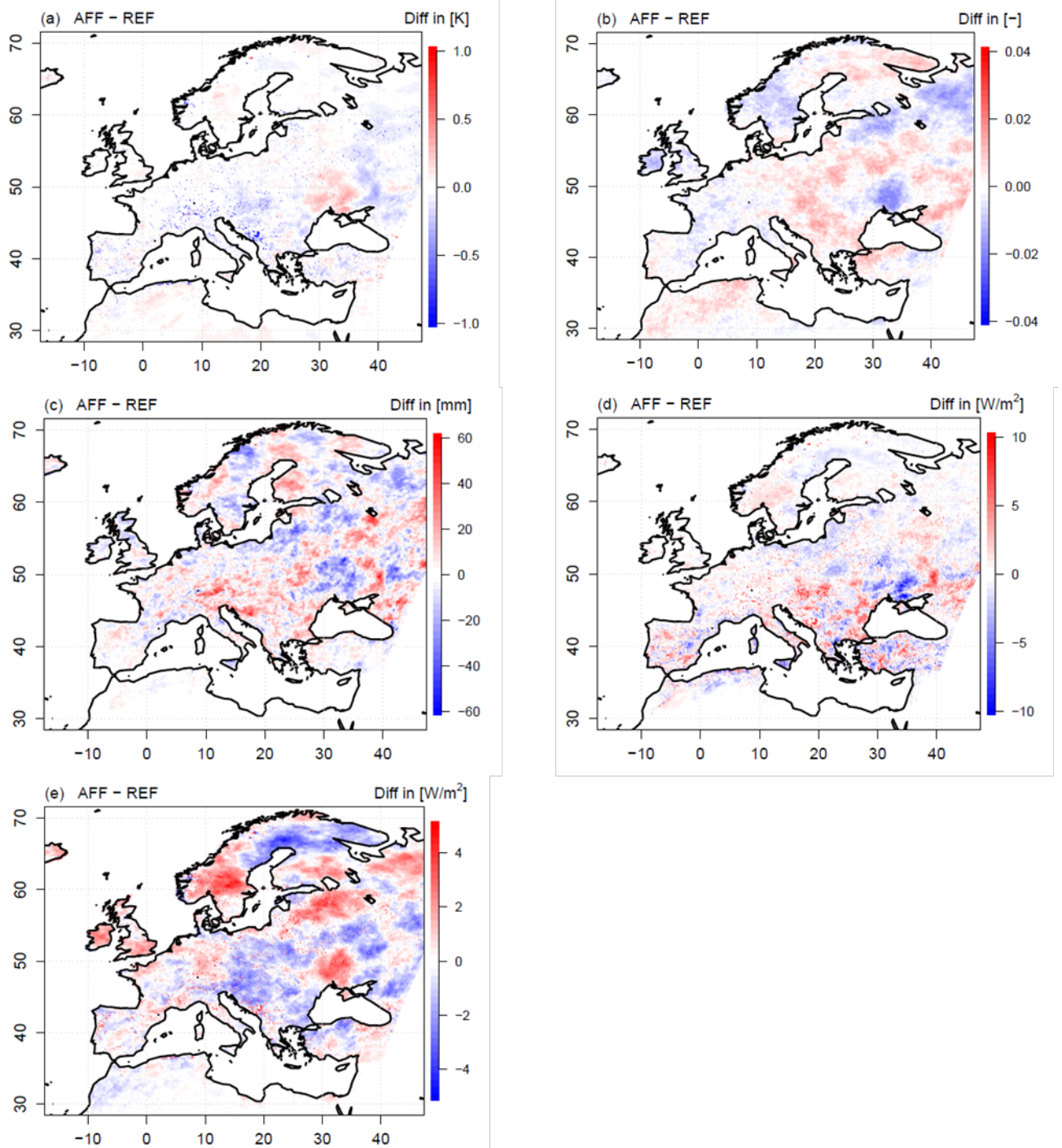
881



882
883

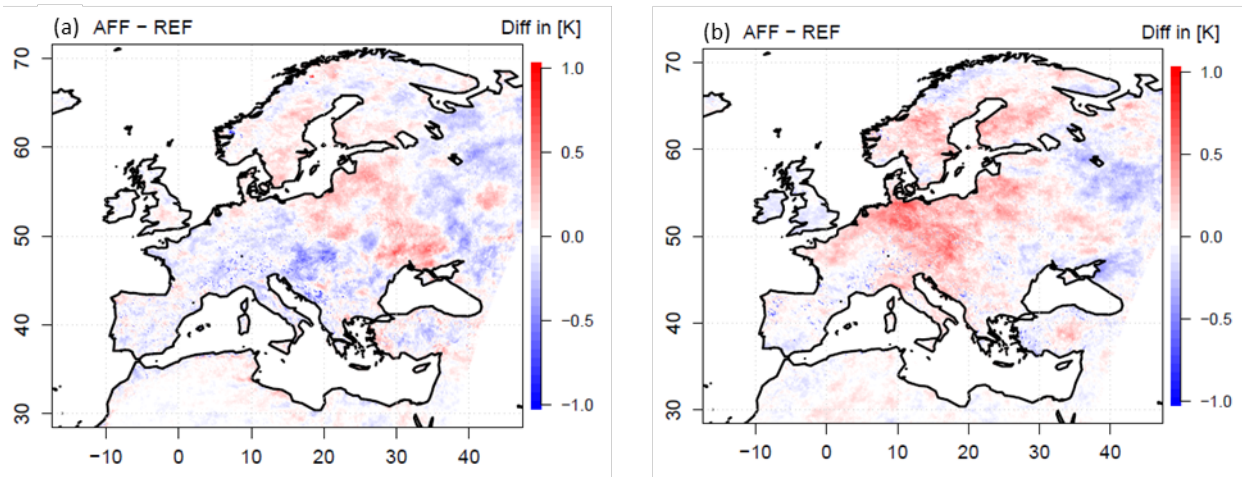
884 Figure 5: Non-local effects of afforestation in Europe on (a) the mean surface temperatures, (b) the
885 mean cloud cover, (c) the mean net short-wave radiation, and (d) the mean net long-wave radiation in
886 winter between AFF and REF.

887
888
889
890
891
892
893
894
895
896
897
898
899
900
901
902
903
904
905
906



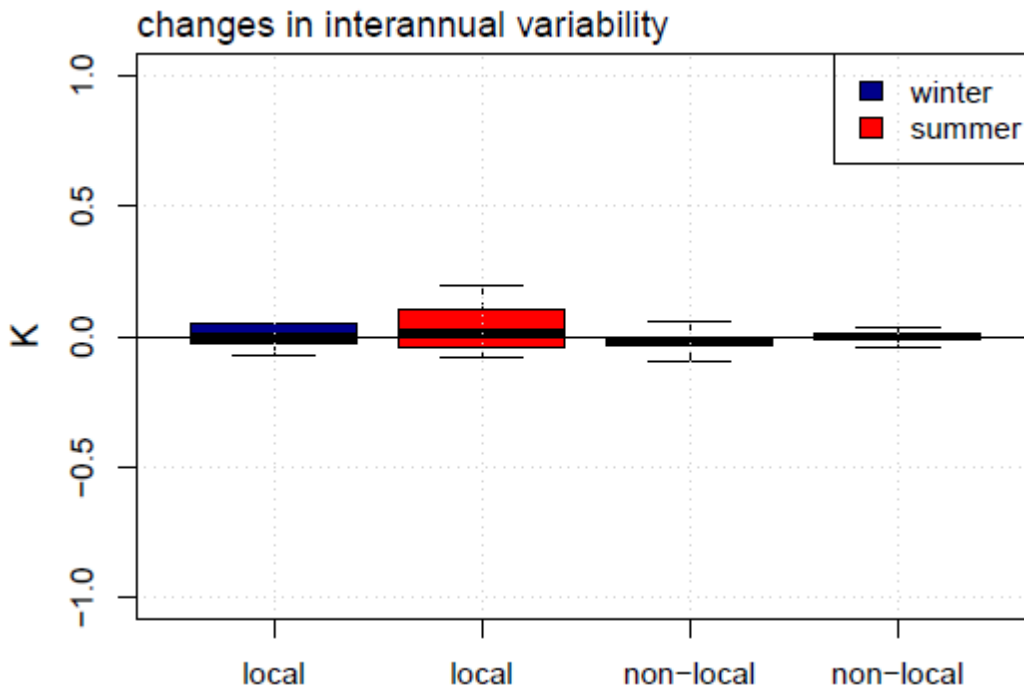
907
 908
 909
 910
 911
 912
 913
 914
 915
 916
 917
 918

Figure 6: Non-local effects of afforestation in Europe on (a) the mean surface temperatures, (b) the mean cloud cover, (c) the mean precipitation sums, (d) the mean evapotranspiration rates, and (e) the mean net short-wave radiation in summer between AFF and REF.



919
 920 Figure 7: Effects of afforestation on temperature extreme intensities in Europe for the period 1986-
 921 2015. Changes in temperature extreme intensities are expressed as the mean temperature differences
 922 in the days (a) above the 90th percentile of the daily maximum temperatures in 2 m height in summer
 923 and (b) below the 10th percentile of the daily maximum temperatures in 2 m height in the winter season
 924 between AFF and REF.

925
 926
 927
 928
 929
 930
 931
 932
 933
 934
 935
 936



937
 938 Figure 8: The effects of afforestation in Europe on the interannual climate variability in winter and
 939 summer for the local and the non-local scales, derived from the standard deviation of the mean
 940 seasonal surface temperatures.

941
 942
 943
 944
 945
 946